Rapid electrochemical detection of COVID-19 genomic sequence with dual-function graphene nanocolloids based biosensor

Wei Li Ang[a], Rachel Rui Xia Lim[a], Adriano Ambrosi[b,c], Alessandra Bonanni[a]*

[a]Division of Chemistry & Biological Chemistry, School of Physical and Mathematical Sciences, Nanyang Technological University, Singapore 637371.

[b]Institute of Materials Research and Engineering, Agency for Science, Technology and Research, Innovis, Singapore 138634, Singapore.

[c]Key Laboratory of Optic-electric Sensing and Analytical Chemistry for Life Science, MOE; Shandong Key Laboratory of Biochemical Analysis; Key Laboratory of Analytical Chemistry for Life Science in Universities of Shandong; College of Chemistry and Molecular Engineering. Qingdao University of Science and Technology, Qingdao 266042, PR China.

Email: a.bonanni@ntu.edu.sg

*Author for correspondence

Abstract

Discovered in December 2019, the Severe Acute Respiratory Syndrome Coronavirus 2 (aka SARS-CoV-2 or 2019-nCoV) has attracted worldwide attention and concerns due to its high transmissibility and the severe health consequences experienced upon its infection, particularly by elderly people. Over 272 million people have been infected till date and over 5.33 million people could not survive the respiratory illness known as COVID-19 syndrome. Rapid and low-cost detection methods are of utmost importance to monitor the diffusion of the virus and to aid in the global fight against the pandemic.

We propose here the use of graphene oxide nanocolloids (GONC) as an electroactive nanocarbon material that can act simultaneously as a transducing platform as well as the electroactive label for the detection of 2019-nCoV genomic sequences. The ability of GONC to provide an intrinsic electrochemical signal arising from the reduction of the electrochemically reducible oxygen functionalities present on its surface, allows GONC to be used as a simple and sensitive biosensing platform. Different intrinsic electroactivity of the material was obtained at each step of the genosensing process, starting from the immobilization of a short-stranded DNA probe and followed by the incubation with different concentrations of the target 2019-nCoV DNA strand. Monitoring such variations enabled the quantification of the target analyte over a wide dynamic range between 10^{-5} M and 10^{-10} M.

All in all, this proof-of-concept system serves as a stepping stone for the development of a rapid, sensitive and selective analytical tool for the detection of 2019-nCoV as well as other similar viral vectors. The use of cost-effective electrochemical detection methods coupled with the vast availability and suitability of carbon-based nanomaterials make this sensing system a valid candidate for low-cost and point-of-care analysis.

Keywords: Genosensor, graphene, electrochemistry, electroactive nanocarbon, SARS-CoV-2, COVID-19.

Introduction

The recent emergence of the novel Severe Acute Respiratory Syndrome Coronavirus 2 (SARS-CoV-2 or 2019-nCoV) has resulted in a widespread pandemic with more than 272 million infections all over the world till date. [1] It has been uncovered, through full-genome sequencing and phylogenetic analysis that the 2019-nCoV possesses features belonging to the coronavirus family as part of the betacoronavirus 2b lineage. [2] Coronaviruses, belonging to the *Coronaviridae* family, are enveloped RNA viruses that possesses the ability to produce respiratory, hepatic, and neurological diseases in humans, mammals, and birds. [3-4] Severe Acute Respiratory Syndrome (SARS-CoV) and Middle East Respiratory Syndrome (MERS-CoV) are two other members of the coronavirus family that have resulted in many fatalities between 2002 and 2003 in China and 2012 in the Middle East respectively. [5-6] Being the seventh member of the coronavirus family, patients diagnosed with 2019-nCoV often experience symptoms that includes fever, fatigue, dry cough and gastrointestinal symptoms, which are similar to that of a seasonal flu and influenza. [7-8] Owing to the difficulty of being able to successfully distinguish between infections of 2019-nCoV and other viral infections from the same *Coronaviridae* family in the early stages, it is of paramount importance to obtain a rapid and specific diagnostic method for the final diagnosis of 2019-nCoV. [9]

Till date, many different detection methods of 2019-nCoV have been reported, with the more commonly utilised methods being classified into either molecular or serological tests. [10-11] Quantitative reverse transcription PCR (RT-qPCR) has been the gold standard method for the detection of 2019-nCoV due to its high sensitivity. However, this method requires the use of bulky equipment and centralized facilities, thereby restricting the possibility of both miniaturisation and *in-situ* testing, [11-14] which would be of utmost importance for mass testing especially in rural areas of developing countries. In addition, serological methods have also been developed where the basis of the detection is dependent on the production of antibodies in the blood serum, that acts specifically against different viral proteins. [15] Unfortunately, antibodies against 2019-nCoV are only developed a few days after clinical manifestations, where the typical incubation period occurs between 3 and 5 days on average. This prevents the development of a rapid immune response, [16-20] making the serological antibody test not suitable for the early detection of COVID-19 infections in order to isolate the infected patients and to block the transmission. [21]

While less accurate antigenic tests based on the detection of viral proteins (known as Antigen Rapid tests-ART) are being developed for mass-screening, [12, 22] the analysis of the genetic material from the virus still remains the method of choice for a reliable detection of an ongoing infection.

Electrochemical detection schemes have shown a great potential in the detection of different viruses and their associated antibodies and antigens, maintaining high sensitivities and selectivities, together with shortened analytical times when compared to the gold standard optical methods. [23-26] The biorecognition of viral proteins, DNA sequences and PCR products correlated to past coronavirus infections have been successfully achieved through electrochemical approaches. Field-effect transistor (FET)-based electrochemical sensors were reported to target the SARS-CoV nucleocapsid (N) protein with sensitivities in the sub-nanomolar concentrations and analysis time of 10 minutes. [27-29] Genome sequences specific to SARS-CoV of 15 to 30-mer length were detected in nanomolar to picomolar range via voltammetry using gold films [30] and screen-printed electrodes. [31-34] Besides SARS-CoV, the detection limit of spike protein (S1) of MERS-CoV have reached a minimum of 1 pg/mL on an array of gold nanoparticles-modified carbon electrodes [35] while that of the amplified PCR products of endemic strains, HCoV-229E and HCoV-OC43 were 128 ng/µL and 760 ng/µL respectively. [36] In response to the current pandemic, novel electrochemical strategies have also emerged in the frontier of COVID-19 diagnostics. A sandwich hybridization assay which integrated isothermal rolling circle amplification with redox-active probes was able to detect copies of N and S genes as low as 1 copy/µL under 2 hours via differential pulse voltammetry (DPV). [37] The newly developed electrochemical immunoassays were able to attain low detection limits for S (19 ng/mL) and N (8 ng/mL) proteins in untreated saliva samples within 30 minutes using DPV as well as 0.1 µg/mL of anti-SARS-CoV-2 IgG antibodies in serum samples under 5 minutes with impedance spectroscopy. [38-39] Parallel to these electrochemical platforms, conductive polymers explored as antifouling electrochemical sensing interface contributed to highly sensitive detection of COVID-19 N-gene in femtomolar scale. [40]

Lately, there has been an upsurge in carbon-based electrochemical biosensors for the detection of various COVID-19 biomarkers, especially focused on graphene nanomaterials. Some of the state-of-the-art graphene-based electrochemical protocols recently developed include a graphene FET functionalized with SARS-CoV-2 spike antibody [41] and complementary phosphorodiamidate morpholino oligos probes, [42] immunoassays embedded with layers of graphene and graphene oxide, [43-46] as well as genosensors based on graphene

nanoplatelets [47] and modified graphene oxide. [48] Among the carbon-based nanomaterials that are currently available, 2D graphene and its derivatives are lightweight, chemically stable, electrically conductive, biocompatible, cost-effective and can be mass produced via facile synthesis from bulk graphite. [49-56] In comparison to carbon nanotubes, graphene does not contain metal impurities that can interfere with electrochemical signals. [53, 55-56] Besides these unique physicochemical properties, a major advantage of utilizing graphene and its derivatives is their high surface area-to-volume ratio for the immobilisation of biomolecules (DNA, protein, enzymes, peptides, antibodies) via covalent or non-covalent bonds such as hydrophobic interactions and π-π stacking. [52-56] Taking advantage of this surface modification, using coupling agent 1-pyrene butyric acid N-hydroxysuccinimide ester (PBASE), Seo *et al*. [41] and Mojsoska *et al.* [43] successfully immobilized SARS-CoV-2 spike antibodies onto the graphene layer to detect SARS-CoV-2 spike protein selectively in clinical samples. In addition, the abundance of reactive oxygen-containing groups (OCGs) present on the surface of graphene oxides, such as hydroxyl, carbonyls, ether and epoxide moieties allow greater ease of functionalisation via physical adsorption, covalent conjugation and affinity binding of the bio-recognition element. [57-61] Owing to the large effective surface area of graphene and its derivatives, higher densities of the receptor immobilised can increase signal-to-noise ratio and give higher analytical sensitivity. As shown in the work by Li *et al.* [42], without the need for amplification, SARS-CoV-2 RdRp gene was detected in femtomolar concentration with morpholino-modified graphene FET-nanosensor. Similarly, Zhao *et al.* [48] were able to obtain 200 SARS-CoV-2 RNA copies/mL with calixarene functionalized graphene oxide that had superior sensitivity over those published RNA detection platforms for SARS-CoV-2.

In view of harnessing the promising capabilities of graphene-based nanomaterials demonstrated in viral sensing, we propose here the development of a nanographene-based biosensor for a simple-to-operate, fast and cost-effective electrochemical detection of 2019-nCoV. We demonstrate the use of the highly electroactive Graphene Oxide Nanocolloids (GONC) as both the immobilisation platform and the signal generation label. [62-63] The rationale behind the design of the biosensor is based on the measurement of the electrochemical signal arising from the reduction of the OCGs present on GONC surface at each step of the genosensing process. The biorecognition element utilised in this study is a short-stranded sequence complementary to the RNA-dependent RNA polymerase (RdRp) genome sequences of SARS-CoV-2. [64] Immobilisation of the biorecognition element onto the surface of GONC via physical adsorption diminishes the number of OCGs available to undergo electrochemical

reduction, which therefore results in an attenuated signal. In the presence of the target analyte (2019-nCoV), the formation of the probe-target complex weakens the non-covalent interactions with the material resulting in a partial detachment of the complex from its surface. The initial electroactivity is thus partially restored as more OCGs are available for electrochemical reduction. Herein, we show how these electrochemical variations can be correlated specifically to different target analyte concentrations as proof-of-concept for the development of a selective and cost effective electrochemical genosensor for the rapid detection of the 2019-nCoV genomic sequences.

Experimental

Materials and Reagents

Graphene Oxide Nanocolloids (GONCs), Sodium Chloride (NaCl), hydrochloric acid and sodium hydroxide were obtained from Sigma Aldrich (Singapore). Sodium phosphate dibasic salt (Na_2HPO_4) was purchased from Merck (Singapore). Trisodium citrate dihydrate was acquired from Alfa Aesar. Disposable electrical printed chips (DEP-Chips) were purchased from BioDevice Technology (Nomi, Japan). Each DEP-Chip consisted of a three-electrode system, including a carbon-based working and counter electrode, as well as an Ag/AgCl reference electrode. PBS (0.01 M Na_2HPO_4, 0.1 M NaCl, pH 7.4), TSC1 (0.075 M Trisodium citrate, 0.75 M NaCl, pH 7) and TSC2 (0.03 M Tris, 0.3 M NaCl, pH 7) buffers were employed for the study. All buffer solutions were prepared with ultrapure water obtained from a Milli-Q ion-exchange column (Millipore) with a resistivity value of 18.2 MΩ/cm. DNA oligonucleotides utilised for the detection of SARS-CoV-2 virus were obtained from Integrated DNA Technologies (IDT) with the following base sequence:

Table 1: Oligonucleotide sequences utilised for SARS-CoV-2 detection in this study

Name	Base Sequence
RdRp-COVID-C (probe)	5'-GCA TCT CCT GAT GAG GTT CCA CCT G-3'
RdRp-COVID (target)	5'-CAG GTG GAA CCT CAT CAG GAG ATG C-3'
RdRp-SARS (mutant)	5'-CCA GGT GGA ACA TCA TCC GGT GAT GC-3'
Non-Complementary (NC)	5'- AAA AAA AAA AAA AAA AAA AAA AAA AA -3'

Stock solutions of DNA oligonucleotides were diluted in sterilized ultrapure water and portioned into aliquots before being stored at -20 °C. A single portion would be defrosted before each usage.

Equipment

Characterisations of GONC was carried out by X-ray Photoelectron Spectroscopy (XPS), Scanning Transmission Electron Microscopy (STEM) and Attenuated Total Reflectance (ATR) spectroscopy. For XPS analysis, several layers of GONC (3 μL for each layer) were drop-casted onto platinum plates before performing the measurements. TEM analysis was performed with JEM 2100F field-emission transmission electron microscope (JEOL, Japan) which

operated at 200 kV. ATR analysis was carried out with a Nicolet iS50R spectrometer (Thermo Scientific, Waltham, MA, USA) and a Smart SAFA specular reflectance accessory. Samples were prepared by drop casting the GONC solution onto a ZnSe crystal.

Electrochemical measurements including Cyclic Voltammetry (CV) and Differential Pulse Voltammetry (DPV) were carried out using a μAutolab type III electrochemical analyser (Eco Chemie, The Netherlands) connected to a computer, and coupled with a GPES software. All electrochemical measurements were performed at room temperature, with PBS functioning as the supporting electrolyte.

A TS-100 Biosan thermoshaker was utilised for temperature-controlled incubations and washing steps between 25–55 °C for 5–30 mins at 300 rpm.

Procedure

GONC suspension from the stock solution was ultrasonicated for 30 minutes before subsequent dilutions to the desired concentration was performed. The diluted GONCs were sonicated for an additional 5 mins before 3 μL of the suspension was deposited onto a bare DEP-Chip and allowed to dry under a lamp. Subsequently, RdRp-COVID-C (probe) was immobilised onto the material film via physical adsorption by drop-casting 3 μL of the solution and drying it at 60 °C for 15 mins. Thereafter, the electrodes were allowed to cool down to room temperature for 5 mins. To remove the excess, non-adsorbed probe, the electrodes were subjected to two washing steps in TSC2 buffer at room temperature with gentle stirring for a duration of 5 mins for each washing step. Next, DEP-Chips modified with DNA probes were incubated in an Eppendorf tube containing the desired concentration of RdRp-COVID (target) in TSC1 buffer. The incubation was performed at 55 °C for 30 mins with gentle stirring. Two brief washing steps were subsequently carried out in TSC2 buffer at 42 °C for 5 mins. All incubations and washing steps were completed using a TS-100 thermoshaker at 300 rpm.

Cyclic Voltammetry (CV) measurements were recorded over a potential range of 0 V to -2 V with a 5 s equilibration time at a scan rate of 20 $mV \cdot s^{-1}$. Differential Pulse Voltammetry (DPV) measurements were obtained from a potential range of 0 V to -2 V at a scan rate of 50 $mV \cdot s^{-1}$ with an equilibration time of 3 seconds, modulation time of 0.05 seconds and modulation amplitude of 0.025 V. All DPV scans were subjected to a moving average baseline correction with a peak width of 0.010.

Results and Discussion

Graphene Oxide Nanocolloids (GONC) are herein employed both as a platform for the immobilisation of the biorecognition element, as well as the electroactive label, capable of providing the electrochemical signal essential for the biosensing process. Being inherently electroactive, GONC offers a large reduction signal arising from the electrochemically reducible oxygen containing groups (OCGs) distributed onto its surface and edges.

Electrochemical characterisation of GONCs was carried out firstly by cyclic voltammetry (CV), in order to confirm the presence of electrochemically reducible OCGs, an essential condition for the material in order to be employed for this study. Figure 1a displays the CV spectra of GONCs scanned over a potential range of 0 V to -2 V. It was observed that a large reduction peak was obtained during the first measured scan, while the signal was no longer present during the second and third scans. This ascertains the presence of a significant amount of electrochemically reducible OCGs and that these were irreversibly fully reduced upon just a single potential scan. [65-66] To gain further insights on the material features, characterisations of GONCs with X-ray Photoelectron Spectroscopy (XPS), Attenuated Total Reflectance (ATR) Spectroscopy and Transmission Electron Microscopy (TEM) was carried out. Figure 1b shows the material structure together with the TEM micrographs displaying well dispersed nanocolloids with an average lateral size in the nanometre range. From the ATR spectra displayed in Figure 1c, peaks corresponding to O-H (3431 cm^{-1}) and C=O (1630 cm^{-1}) stretching modes could be correlated to the presence of carbonyl, hydroxyls and carboxylic groups respectively, while peaks corresponding to C-O (1252 cm^{-1}) stretching mode belonged to epoxides and ethers. Additionally, peaks of C-H (2919 cm^{-1}) and C=C (1572 cm^{-1}) stretching modes were observed, which can be correlated to the sp^2 conjugated network of graphene. From the XPS survey scan in Figure 1d, a C/O ratio value of 1.79 was attained, a value considerably lower than the typical characteristic value range of 2.00 to 4.00 for GOs, [67] confirming a high degree of oxidation and abundance of oxygen groups. This can be attributed to the small lateral dimension (nanometre scale) which produces a high density of oxygenated species. The deconvoluted high resolution C1s spectra resulted in four distinct peaks occurring at different binding energies. The peak occurring at 284.4 eV is associated with the C=C aromatic rings of the sp^2 graphene sheets while the peaks observed at 285.5 and 286.5 eV corresponded to the C-O single bond, and C=O double bond found in carbonyl moieties respectively. Lastly, the peak attained at 288.8 eV belongs to the carboxyl groups present in carboxylic acids.

Overall, the obtained results from ATR and XPS confirm the suitability of the material for this study, owing to the highly oxidised GONC surface, corresponding to a high inherent electroactivity of the nanomaterial.

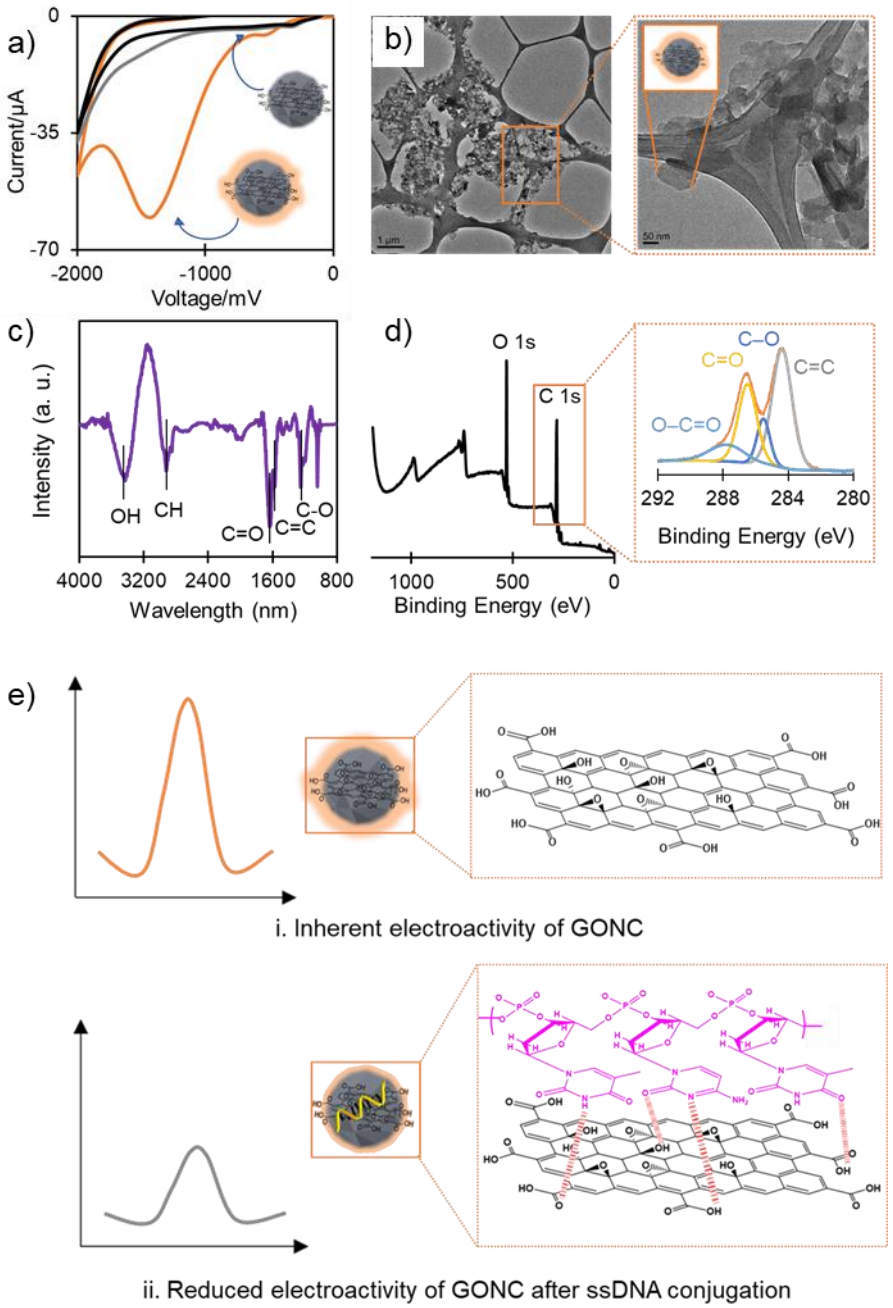

Figure 1. Characterization of GONCs. a) Electrochemical characterization by cyclic voltammetry; b) TEM Micrograph with scale bar of 1 µm and 50 nm respectively; c) Attenuated Total Reflectance Spectra – ATR; d) X-Ray Photoelectron Spectroscopy survey spectrum and deconvoluted high resolution C1s spectra; e) General scheme depicting the use of GONCs as platform and label for the development of a genosensor for the detection of SARS-CoV-2

genome. i. The inherent electroactivity of GONC is first measured, with the electrochemical peak recorded (orange color) corresponding to the reduction of OCGs on the material surface; ii. After the immobilization of SARS-CoV-2 cDNA, a reduced electroactivity is shown by GONCs (grey color).

Following the characterizations performed, GONC was utilized as an electroactive platform for the detection of SARS-CoV-2 related sequences. The detection principle for this study is displayed in Figure 1e. GONC intrinsic electroactivity is first monitored by differential pulse voltammetry (DPV), showing a reduction peak due to the presence of electrochemically reducible OCGs. Upon RdRp-COVID-C (probe) immobilization onto the GONC surface via physical adsorption, the non-covalent interactions formed reduce the availability of OCGs for electrochemical reduction. This results in a diminished inherent electroactivity of the material, with a signal suppression recorded.

Thereafter, three hybridization experiments were carried out to clearly illustrate the biosensing principle. The electrode modified with the RdRp-COVID-C (probe) was incubated in three different solutions containing: i) the complementary RdRp-COVID (target) oligonucleotide; ii) a three-base mismatch RdRp-SARS (mutant) oligonucleotide and iii) a non-complementary (NC) oligonucleotide

As illustrated in Figure 2a, the intrinsic electroactivity of GONC arising from the reduction of the electrochemically reducible OCGs on the material surface was first measured by differential pulse voltammetry (DPV) (red line). Subsequent immobilization of the DNA probe onto the GONC modified electrodes was performed, and a significant decrease in the electrochemical signal was observed (blue line). This phenomenon can be correlated to the formation of non-covalent interactions including hydrogen bonding, hydrophobic interactions as well as π- π stacking interactions between the GONC surface and the DNA nucleobases. [68-69] Thereafter, hybridization of the GONC-probe modified electrodes with RdRp-COVID complementary target showed a restoration of the electrochemical signal owing to the partial detachment of the formed probe-target complex from the GONC surface. This is due to fact that graphene materials form stronger interactions with ssDNA molecules compared to dsDNA. [55, 70] As a result, an increased number of OCGs are available for reduction, thereby partially restoring the inherent electroactivity of the GONCs (yellow line). Control experiments with non-complementary and three-base mismatch sequence oligonucleotides further confirms the validity of this mechanism as illustrated in Figure 2b. It can be observed that in the presence

of oligonucleotides with non-complementary (NC) or minimal mismatches (mutant) sequences, an opposite trend is recorded confirming that not only the probe molecule remains attached onto the material, but that more interactions are generated by the added oligonucleotides which further suppress the electrochemical signal. This results confirms a high level of selectivity of the developed protocol for the detection of RdRp-COVID specific sequence.

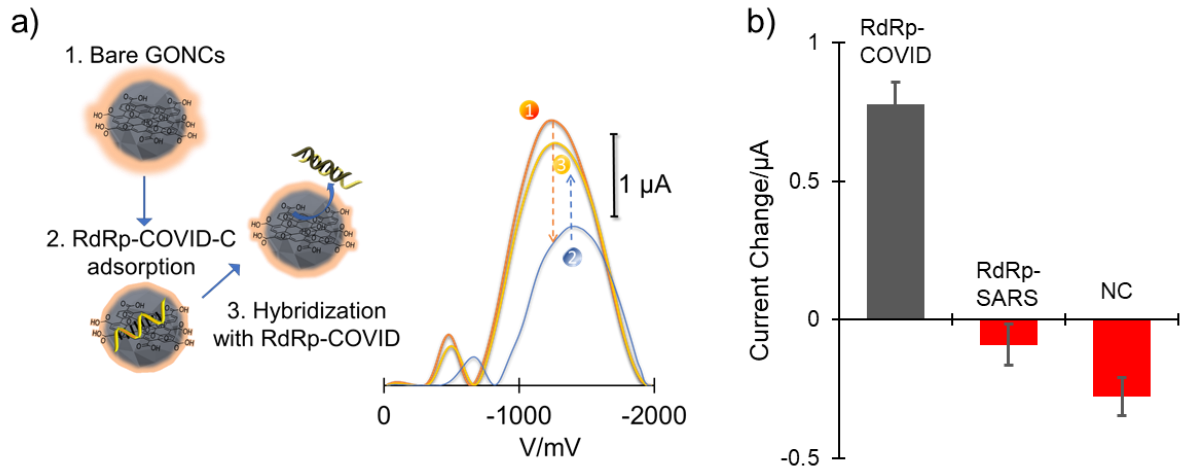

Figure 2. Preliminary experiment displaying: a) The schematic of the biosensing and the differential pulse voltammograms for: bare GONCs (1); RdRp COVID-C modified GONCs (2); Hybridization with RdRp-COVID (3); b) Histograms of the electrochemical response for different hybridization experiments with: RdRp-COVID (complementary target); RdRp-SARS (mutant with 3-base mismatch); Non-complementary target (NC). Concentration of target analytes: 1×10^{-7} M; Current Change represent the difference between signals obtained with RdRp COVID-C modified GONCs and the target analytes.

Having demonstrated the capability of GONC to function simultaneously as both platform and electrochemical label, optimisation of the developed platform was subsequently carried out. As a result, different concentrations of the DNA probe, functioning as the biorecognition element of the geno-assay were examined, in a bid to determine the optimum concentration of DNA probe to be immobilised onto the surface of GONC so as to reduce the probability of non-specific adsorptions. To this aim, two different techniques were utilised for this study: differential pulse voltammetry (DPV) and electrochemical impedance spectroscopy (EIS). From Figure 3a, the histogram was obtained following the immobilisation of the DNA probe onto the GONC surface (left side). The results shown indicate a decrease in the magnitude of the current with increasing concentrations of the DNA probe, ranging from 0.01 µM to 200 µM. The corresponding relevant voltammogram was also displayed in Figure 3a (right side). For the whole set of voltammograms please refer to Figure S1 of Supporting Information.

Subsequently, to further ascertain the optimal concentration of the DNA probe, a similar study was conducted with EIS with the obtained results displayed in the form of a histogram in Figure 3b (left side). It was uncovered that a larger R_{CT} value was observed with increasing concentrations of the DNA probe. This phenomenon could be attributed to the electrostatic repulsion between the negative charges present on the phosphate backbone of the DNA probe and the negatively charged $[Fe(CN)_6]^{3-/4-}$ redox probe, thereby hindering the electron transfer process. Therefore, an increase in the magnitude of the impedimetric signal is indicative of the amount of DNA probe that has been successfully immobilised onto the GONC surface, with a larger increase in the R_{CT} value equivalent to a larger amount of immobilised DNA. Noticeably, 100 μM of DNA probe offered the largest increase in the R_{CT} value and was therefore chosen as the optimal concentration of the biorecognition element to ensure maximum coverage of the GONC surface. For reference, the corresponding relevant Nyquist plots obtained from the EIS study was also displayed (Figure 3b, right side). For the whole set of Nyquist plots, please refer to Figure S2 of Supporting Information.

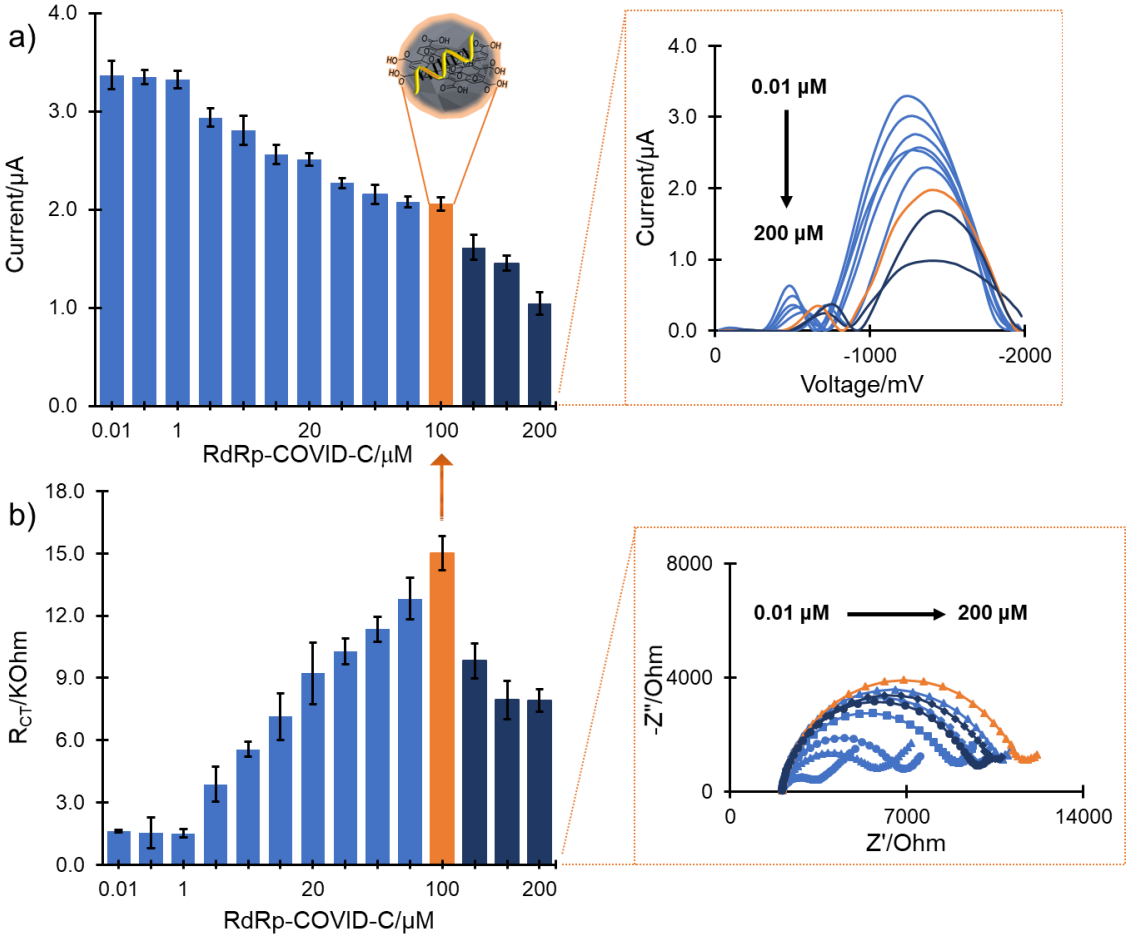

Figure 3. Optimisation of the RdRp-COVID-C concentration: a) Bar chart and voltammograms representing the peak current towards the reduction of electrochemically reducible OCGs present on the GONC surface with varying RdRp-COVID-C concentrations and using differential pulse voltammetry. Conditions: 0.1 M PBS buffer, pH 7.0. b) Bar chart and Nyquist plots representing the variation in the charge transfer resistance (R_{CT}) towards increasing RdRp-COVID-C concentrations. Conditions: 0.1 M PBS buffer, pH 7.0, containing10 mM ferrocyanide/ferricyanide (1:1 molar ratio).

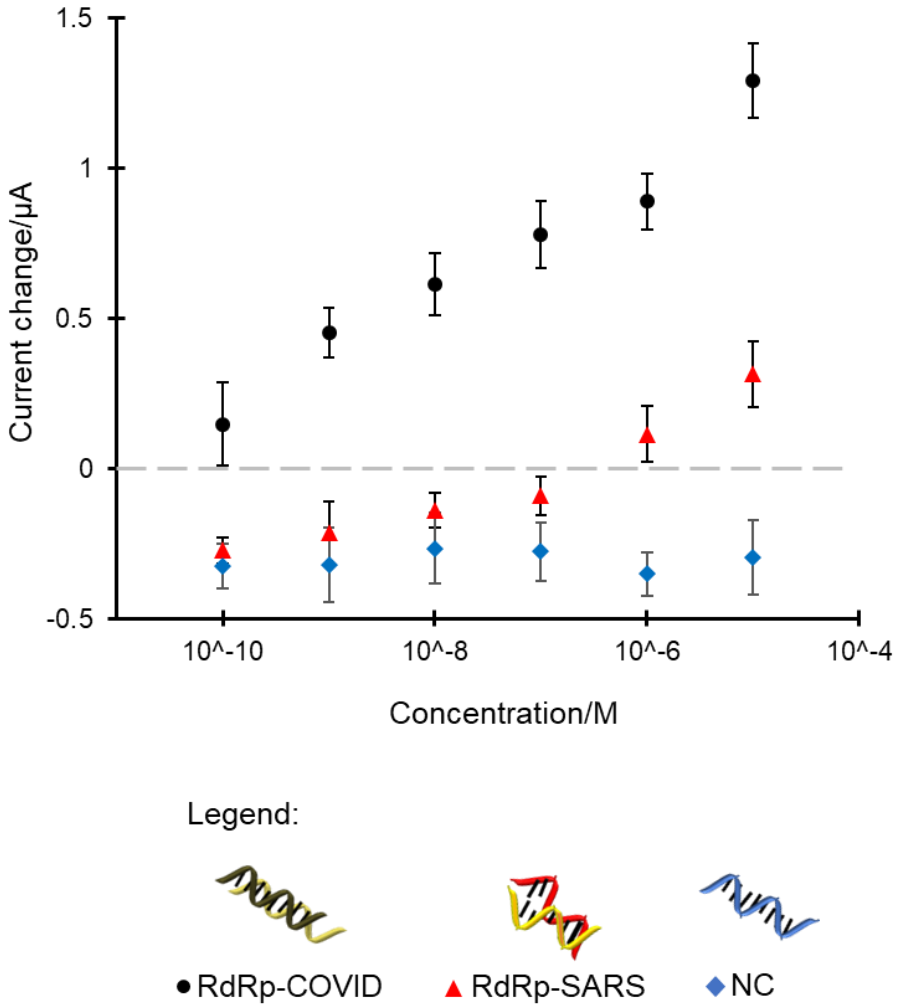

Figure 4. Variations in the voltammetric peak currents of the genosensor with different hybridisation targets ranging from 10^{-10} M to 10^{-5} M: a) RdRp-COVID complementary target (black circles) and RdRp-SARS mutant sequence (red triangles); b) RdRp-COVID complementary target (black circles) and non-complementary sequence (blue diamonds). Error bars represent the standard deviation of five independent experiments. Current Change represent the difference between signals obtained with RdRp COVID-C modified GONCs and the target analytes.

Moving on, a calibration experiment was performed with increasing concentrations of the RdRp-COVID complementary target to calculate the variations of the electrochemical signal in order to evaluate the detection range for the GONC platform. To this aim, 100 μM of the RdRp-COVID-C probe was immobilised onto GONC surface before further incubation with the RdRp-COVID complementary target (ranging from 10^{-10} M to 10^{-5} M). The resultant reduction signal was monitored and displayed in Figure 4a. From the obtained results, a more

significant signal restauration was recorded for increasing concentrations of RdRp-COVID complementary target, while for hybridization with the the three-base mismatch RdRp-SARS mutant sequence (red triangles in Figure 4a), and a non-complementary (NC) sequence (blue diamonds in Figure 4b), the signal restoration recorded was negligible.

Lastly, the linear dynamic range of the geno-assay was found to be between 10^{-10} and 10^{-5} M. The limits of detection was determined to be approximately 186×10^{-9} M, calculated by taking into account three times the standard deviation of the population of blank responses and the slope of the regression line. [71]

Conclusion

This study shows the possibility of employing GONCs as the electroactive nanomaterial owing to the dual function it possesses, as both a transducing platform and an electroactive label for the detection of 2019-nCoV target sequences. This alternative detection approach is based on the variations of the electrochemical signal arising from the electrochemically reducible oxygen containing groups present on the GONC surface. Specifically, immobilisation of the DNA probe, functioning as the biorecognition element, onto the GONC platform would result in a reduction of the initial electrochemical signal, which is later partially restored in the presence of the 2019-nCoV target. Owing to the formation of the probe-target conjugate, this results in a partial detachment of the formed conjugate from the platform. Herein, we have also established a direct correlation between the electrochemical signal arising from the inherent electroactivity of GONC and the 2019-nCoV concentration over a wide linear range from 10^{-10} to 10^{-5} M. In addition, we have also demonstrated high selectivity for the proposed geno-assay with negligible interference for the SARS-CoV target, a virus belonging to the same coronavirus family as 2019-nCoV. The proposed detection technique could be integrated in a DNA amplifier for the portable and low-cost identification of 2019-nCoV virus in infected patients, without the need to carry the sample to lab-centralized facilities.

Acknowledgements

A.B. acknowledges Ministry of Education (MOE), AcRF Tier 1 grant (Reference No: RG88/20) for the financial support. A.A. acknowledges the support of the Double-Hundred Program for Foreign Experts of Shandong Province (WST2019011).

References

[1] John Hopkins University of Medicine, Coronavirus Statistics. https://coronavirus.jhu.edu/, 2021 (accesed 17 December 2021).

[2] N. Zhu, D. Zhang, W. Wang, X. Li, B. Yang, J. Song, X. Zhao, B. Huang, W. Shi, R. Lu, P. Niu, F. Zhan, X. Ma, D. Wang, W. Xu, G. Wu, G. F. Gao, W. Tan, A Novel Coronavirus from Patients with Pneumonia in China, 2019, N. Engl. J. Med. 382 (8) (2020) 727-733.

[3] S. R. Weiss, J. L. Leibowitz, Coronavirus pathogenesis, Adv. Virus Res. 81 (2011) 85-164.

[4] K. V. Holmes, Encyclopedia of Virology, second ed., Elseiver, 1999.

[5] M. A. Shereen, S. Khan, A. Kazmi, N. Bashir, R. Siddique, COVID-19 infection: Origin, transmission, and characteristics of human coronaviruses, J. Adv. Res. 24 (2020) 91-98.

[6] M. Feng, J. Chen, J. Xun, R. Dai, W. Zhao, H. Lu, J. Xu, L. Chen, G. Sui, X. Cheng, Development of a Sensitive Immunochromatographic Method Using Lanthanide Fluorescent Microsphere for Rapid Serodiagnosis of COVID-19, ACS Sens. 5 (8) (2020) 2331-2337.

[7] M. Cao, D. Zhang, Y. Wang, Y. Lu, X. Zhu, Y. Li, H. Xue, Y. Lin, M. Zhang, Y. Sun, Z. Yang, J. Shi, Y. Wang, C. Zhou, Y. Dong, P. Liu, S. M. Dudek, Z. Xiao, H. Lu, L. Peng, Clinical Features of Patients Infected with the 2019 Novel Coronavirus (COVID-19) in Shanghai, China, medRxiv. 2020) 2020.2003.2004.20030395.

[8] N. Chen, M. Zhou, X. Dong, J. Qu, F. Gong, Y. Han, Y. Qiu, J. Wang, Y. Liu, Y. Wei, J. Xia, T. Yu, X. Zhang, L. Zhang, Epidemiological and clinical characteristics of 99 cases of 2019 novel coronavirus pneumonia in Wuhan, China: a descriptive study, Lancet. 395 (10223) (2020) 507-513.

[9] M. J. Loeffelholz, Y. W. Tang, Laboratory diagnosis of emerging human coronavirus infections - the state of the art, Emerg. Microbes Infect. 9 (1) (2020) 747-756.

[10] P. Moitra, M. Alafeef, K. Dighe, M. B. Frieman, D. Pan, Selective Naked-Eye Detection of SARS-CoV-2 Mediated by N Gene Targeted Antisense Oligonucleotide Capped Plasmonic Nanoparticles, ACS Nano. 14 (6) (2020) 7617-7627.

[11] J. Wang, K. Cai, R. Zhang, X. He, X. Shen, J. Liu, J. Xu, F. Qiu, W. Lei, J. Wang, X. Li, Y. Gao, Y. Jiang, W. Xu, X. Ma, Novel One-Step Single-Tube Nested Quantitative Real-Time PCR Assay for Highly Sensitive Detection of SARS-CoV-2, Anal. Chem. 92 (13) (2020) 9399-9404.

[12] P. Mertens, N. De Vos, D. Martiny, C. Jassoy, A. Mirazimi, L. Cuypers, S. Van den Wijngaert, V. Monteil, P. Melin, K. Stoffels, N. Yin, D. Mileto, S. Delaunoy, H. Magein, K. Lagrou, J. Bouzet, G. Serrano, M. Wautier, T. Leclipteux, M. Van Ranst, O. Vandenberg, L.-U. S.-C.-W. D. G. , B. Gulbis, F. Brancart, F. Bry, B. Cantinieaux, F. Corazza, F. Cotton, M. Dresselhuis, B. Mahadeb, O. Roels, J. Vanderlinden, Development and Potential Usefulness of the COVID-19 Ag Respi-Strip Diagnostic Assay in a Pandemic Context, Front. Med. 7 (225) (2020).

[13] J. P. Broughton, X. Deng, G. Yu, C. L. Fasching, V. Servellita, J. Singh, X. Miao, J. A. Streithorst, A. Granados, A. Sotomayor-Gonzalez, K. Zorn, A. Gopez, E. Hsu, W. Gu, S. Miller, C. Y. Pan, H. Guevara, D. A. Wadford, J. S. Chen, C. Y. Chiu, CRISPR-Cas12-based detection of SARS-CoV-2, Nat. Biotechnol. 38 (2020) 870-874.

[14] L. Wang, Y. Wang, D. Ye, Q. Liu, Review of the 2019 novel coronavirus (SARS-CoV-2) based on current evidence, Int. J. Antimicrob. Agents. 55 (6) (2020) 105948.

[15] R. Kubina, A. Dziedzic, Molecular and Serological Tests for COVID-19 a Comparative Review of SARS-CoV-2 Coronavirus Laboratory and Point-of-Care Diagnostics, Diagnostics. 10 (6) (2020) 434.

[16] Q.-X. Long, B.-Z. Liu, H.-J. Deng, G.-C. Wu, K. Deng, Y.-K. Chen, P. Liao, J.-F. Qiu, Y. Lin, X.-F. Cai, D.-Q. Wang, Y. Hu, J.-H. Ren, N. Tang, Y.-Y. Xu, L.-H. Yu, Z. Mo, F. Gong, X.-L. Zhang, W.-G. Tian, L. Hu, X.-X. Zhang, J.-L. Xiang, H.-X. Du, H.-W. Liu, C.-H. Lang, X.-H. Luo, S.-B. Wu, X.-P. Cui, Z. Zhou, M.-M. Zhu, J. Wang, C.-J. Xue, X.-F. Li, L. Wang, Z.-J. Li, K. Wang, C.-C. Niu, Q.-J. Yang, X.-J. Tang, Y. Zhang, X.-M. Liu, J.-J. Li, D.-C. Zhang, F. Zhang, P. Liu, J. Yuan, Q. Li, J.-L. Hu, J. Chen, A.-L. Huang, Antibody responses to SARS-CoV-2 in patients with COVID-19, Nat. Med. 26 (6) (2020) 845-848.

[17] S. A. Lauer, K. H. Grantz, Q. Bi, F. K. Jones, Q. Zheng, H. R. Meredith, A. S. Azman, N. G. Reich, J. Lessler, The Incubation Period of Coronavirus Disease 2019 (COVID-19) From Publicly Reported Confirmed Cases: Estimation and Application, Ann. Intern. Med. 172 (9) (2020) 577-582.

[18] G. Caruana, A. Croxatto, A. T. Coste, O. Opota, F. Lamoth, K. Jaton, G. Greub, Diagnostic strategies for SARS-CoV-2 infection and interpretation of microbiological results, Clin. Microbiol. Infect. 26 (9) (2020) 1178-1182.
[19] J. Zhao, Q. Yuan, H. Wang, W. Liu, X. Liao, Y. Su, X. Wang, J. Yuan, T. Li, J. Li, S. Qian, C. Hong, F. Wang, Y. Liu, Z. Wang, Q. He, Z. Li, B. He, T. Zhang, Y. Fu, S. Ge, L. Liu, J. Zhang, N. Xia, Z. Zhang, Antibody Responses to SARS-CoV-2 in Patients With Novel Coronavirus Disease 2019, Clin. Infect. Dis. 2020).
[20] R. T. Suhandynata, M. A. Hoffman, M. J. Kelner, R. W. McLawhon, S. L. Reed, R. L. Fitzgerald, Longitudinal Monitoring of SARS-CoV-2 IgM and IgG Seropositivity to Detect COVID-19, J. Appl. Lab Med. 5 (5) (2020) 908-920.
[21] FierceBiotech, Current COVID-19 antibody tests aren't accurate enough for mass screening, say Oxford researchers. https://www.fiercebiotech.com/medtech/current-covid-19-antibody-tests-aren-t-accurate-enough-for-mass-screening-say-oxford, 2020 (accesed 31 August 2020).
[22] V. M. Corman, V. C. Haage, T. Bleicker, M. L. Schmidt, B. Muhlemann, M. Zuchowski, W. K. Jo, P. Tscheak, E. Moncke-Buchner, M. A. Muller, A. Krumbholz, J. F. Drexler, C. Drosten, Comparison of seven commercial SARS-CoV-2 rapid point-of-care antigen tests: a single-centre laboratory evaluation study, Lancet Microbe. 2 (7) (2021) E311-E319.
[23] R. R. X. Lim, A. Bonanni, The potential of electrochemistry for the detection of coronavirus-induced infections, Trends Anal. Chem. 133 (2020) 116081.
[24] M. Z. H. Khan, M. R. Hasan, S. I. Hossain, M. S. Ahommed, M. Daizy, Ultrasensitive detection of pathogenic viruses with electrochemical biosensor: State of the art, Biosens. Bioelectron. 166 (2020) 112431.
[25] M. R. de Eguilaz, L. R. Cumba, R. J. Forster, Electrochemical detection of viruses and antibodies: A mini review, Electrochem. Commun. 116 (2020) 106762.
[26] G. Balkourani, A. Brouzgou, M. Archonti, N. Papandrianos, S. Song, P. Tsiakaras, Emerging materials for the electrochemical detection of COVID-19, J. Electroana.l Chem. 893 (2021) 115289.
[27] F. N. Ishikawa, H. K. Chang, M. Curreli, H. I. Liao, C. A. Olson, P. C. Chen, R. Zhang, R. W. Roberts, R. Sun, R. J. Cote, M. E. Thompson, C. Zhou, Label-Free, Electrical Detection of the SARS Virus N-Protein with Nanowire Biosensors Utilizing Antibody Mimics as Capture Probes, ACS Nano. 3 (2009) 1219–1224.
[28] F. N. Ishikawa, M. Curreli, C. A. Olson, H. I. Liao, R. Sun, R. W. Roberts, R. J. Cote, M. E. Thompson, C. Zhou, Importance of Controlling Nanotube Density for Highly Sensitive and Reliable Biosensors Functional in Physiological Conditions, ACS Nano. 4 (2010) 6914–6922.
[29] Y.-R. Hsu, G.-Y. Lee, J.-I. Chyi, C.-k. Chang, C.-C. Huang, C.-P. Hsu, T.-h. Huang, F. Ren, Y.-L. Wang, Detection of Severe Acute Respiratory Syndrome Coronavirus Using AlGaN GaN High Electron Mobility Transistors, ECS Trans. 50 (6) (2012) 239-243.
[30] P. Abad-Valle, M. T. Fernandez-Abedul, A. Costa-Garcia, Genosensor on gold films with enzymatic electrochemical detection of a SARS virus sequence, Biosens. Bioelectron. 20 (11) (2005) 2251-2260.
[31] G. Martínez-Paredes, M. B. González-García, A. Costa-García, Genosensor for SARS Virus Detection Based on Gold Nanostructured Screen-Printed Carbon Electrodes, Electroanalysis. 21 (3-5) (2009) 379-385.
[32] P. Abad-Valle, M. T. Fernandez-Abedul, A. Costa-Garcia, DNA single-base mismatch study with an electrochemical enzymatic genosensor, Biosens. Bioelectron. 22 (8) (2007) 1642-1650.
[33] M. Diaz-Gonzalez, A. de la Escosura-Muniz, M. B. Gonzalez-Garcia, A. Costa-Garcia, DNA hybridization biosensors using polylysine modified SPCEs, Biosens. Bioelectron. 23 (9) (2008) 1340-1346.
[34] R. Garcia-Gonzalez, A. Costa-Garcia, M. T. Fernandez-Abedul, Methylene blue covalently attached to single stranded DNA as electroactive label for potential bioassays, Sens. Actuators B Chem. 191 (2014) 784-790.
[35] L. A. Layqah, S. Eissa, An electrochemical immunosensor for the corona virus associated with the Middle East respiratory syndrome using an array of gold nanoparticle-modified carbon electrodes, Mikrochim. Acta. 186 (4) (2019) 224.
[36] M. J. Lodes, D. Suciu, J. L. Wilmoth, M. Ross, S. Munro, K. Dix, K. Bernards, A. G. Stover, M. Quintana, N. Iihoshi, W. J. Lyon, D. L. Danley, A. McShea, Identification of upper respiratory tract

pathogens using electrochemical detection on an oligonucleotide microarray, PLoS One. 2 (9) (2007) e924.
[37] T. Chaibun, J. Puenpa, T. Ngamdee, N. Boonapatcharoen, P. Athamanolap, A. P. O'Mullane, S. Vongpunsawad, Y. Poovorawan, S. Y. Lee, B. Lertanantawong, Rapid electrochemical detection of coronavirus SARS-CoV-2, Nat. Commun. 12 (802) (2021).
[38] L. Fabiani, M. Saroglia, G. Galatà, R. De Santis, S. Fillo, V. Luca, G. Faggioni, N. D'Amore, E. Regalbuto, P. Salvatori, G. Terova, D. Moscone, F. Lista, F. Arduini, Magnetic beads combined with carbon black-based screen-printed electrodes for COVID-19: A reliable and miniaturized electrochemical immunosensor for SARS-CoV-2 detection in saliva, Biosens. Bioelectron. 171 (2021) 112686.
[39] M. Z. Rashed, J. A. Kopechek, M. C. Priddy, K. T. Hamorsky, K. E. Palmer, N. Mittal, J. Valdez, J. Flynn, S. J. Williams, Rapid detection of SARS-CoV-2 antibodies using electrochemical impedance-based detector, Biosens. Bioelectron. 171 (2021) 112709.
[40] Z. Song, Y. Ma, M. Chen, A. Ambrosi, C. Ding, X. Luo, Electrochemical Biosensor with Enhanced Antifouling Capability for COVID-19 Nucleic Acid Detection in Complex Biological Media, Anal. Chem. 93 (14) (2021) 5963-5971.
[41] G. Seo, G. Lee, M. J. Kim, S. H. Baek, M. Choi, K. B. Ku, C. S. Lee, S. Jun, D. Park, H. G. Kim, S. J. Kim, J. O. Lee, B. T. Kim, E. C. Park, S. I. Kim, Rapid Detection of COVID-19 Causative Virus (SARS-CoV-2) in Human Nasopharyngeal Swab Specimens Using Field-Effect Transistor-Based Biosensor, ACS Nano. 14 (4) (2020) 5135-5142.
[42] J. Li, D. Wu, Y. Yu, T. Li, K. Li, M. M. Xiao, Y. Li, Z. Y. Zhang, G. J. Zhang, Rapid and unamplified identification of COVID-19 with morpholino-modified graphene field-effect transistor nanosensor, Biosens. Bioelectron. 183 (2021) 113206.
[43] B. Mojsoska, S. Larsen, D. A. Olsen, J. S. Madsen, I. Brandslund, F. A. Alatraktchi, Rapid SARS-CoV-2 Detection Using Electrochemical Immunosensor, Sensors. 21 (2) (2021).
[44] R. M. Torrente-Rodriguez, H. Lukas, J. Tu, J. Min, Y. Yang, C. Xu, H. B. Rossiter, W. Gao, SARS-CoV-2 RapidPlex: A Graphene-Based Multiplexed Telemedicine Platform for Rapid and Low-Cost COVID-19 Diagnosis and Monitoring, Matter. 3 (6) (2020) 1981-1998.
[45] A. Yakoh, U. Pimpitak, S. Rengpipat, N. Hirankarn, O. Chailapakul, S. Chaiyo, Paper-based electrochemical biosensor for diagnosing COVID-19: Detection of SARS-CoV-2 antibodies and antigen, Biosens. Bioelectron. 176 (2021) 112912.
[46] M. A. Ali, C. Hu, S. Jahan, B. Yuan, M. S. Saleh, E. Ju, S. J. Gao, R. Panat, Sensing of COVID-19 Antibodies in Seconds via Aerosol Jet Nanoprinted Reduced-Graphene-Oxide-Coated 3D Electrodes, Adv. Mater. 33 (7) (2021) e2006647.
[47] M. Alafeef, K. Dighe, P. Moitra, D. Pan, Rapid, Ultrasensitive, and Quantitative Detection of SARS-CoV-2 Using Antisense Oligonucleotides Directed Electrochemical Biosensor Chip, ACS Nano. 14 (2020) 17028-17045.
[48] H. Zhao, F. Liu, W. Xie, T. C. Zhou, J. OuYang, L. Jin, H. Li, C. Y. Zhao, L. Zhang, J. Wei, Y. P. Zhang, C. P. Li, Ultrasensitive supersandwich-type electrochemical sensor for SARS-CoV-2 from the infected COVID-19 patients using a smartphone, Sens. Actuators B Chem. 327 (2021) 128899.
[49] W. S. Hummers, R. E. Offeman, Preparation of Graphitic Oxide, J. Am. Chem. Soc. 80 (6) (1958) 1339-1339.
[50] L. Staudenmaier, Verfahren zur Darstellung der Graphitsäure, Ber. Dtsch. Chem. Ges. 31 (2) (1898) 1481-1487.
[51] U. Hofmann, E. Konig, Analysis on graphite dioxide, Z. Anorg. Allg. Chem. 234 (4) (1937) 311-336.
[52] E. Vermisoglou, D. Panáček, K. Jayaramulu, M. Pykal, I. Frébort, M. Kolář, M. Hajdúch, R. Zbořil, M. Otyepka, Human virus detection with graphene-based materials, Biosens. Bioelectron. 166 (2020) 112436.
[53] C. I. L. Justino, A. R. Gomes, A. C. Freitas, A. C. Duarte, T. A. P. Rocha-Santos, Graphene based sensors and biosensors, Trends Anal. Chem. 91 (2017) 53-66.
[54] D. Chen, H. Feng, J. Li, Graphene oxide: preparation, functionalization, and electrochemical applications, Chem. Rev. 112 (11) (2012) 6027-6053.
[55] Z. Jiang, B. Feng, J. Xu, T. Qing, P. Zhang, Z. Qing, Graphene biosensors for bacterial and viral pathogens, Biosens. Bioelectron. 166 (2020) 112471.

[56] F. Liu, K. S. Choi, T. J. Park, S. Y. Lee, T. S. Seo, Graphene-based electrochemical biosensor for pathogenic virus detection, Biochip J. 5 (2) (2011) 123-128.
[57] S. S. Nanda, G. C. Papaefthymiou, D. K. Yi, Functionalization of Graphene Oxide and its Biomedical Applications, Crit. Rev. Solid State Mater. Sci. 40 (5) (2015) 291-315.
[58] H. Wang, Q. Zhang, X. Chu, T. Chen, J. Ge, R. Yu, Graphene Oxide–Peptide Conjugate as an Intracellular Protease Sensor for Caspase-3 Activation Imaging in Live Cells, Angew. Chem. Int. Ed. 50 (31) (2011) 7065-7069.
[59] J. Lu, L. T. Drzal, R. M. Worden, I. Lee, Simple Fabrication of a Highly Sensitive Glucose Biosensor Using Enzymes Immobilized in Exfoliated Graphite Nanoplatelets Nafion Membrane, Chem. Mater. 19 (25) (2007) 6240-6246.
[60] H. Chang, L. Tang, Y. Wang, J. Jiang, J. Li, Graphene Fluorescence Resonance Energy Transfer Aptasensor for the Thrombin Detection, Anal. Chem. 82 (6) (2010) 2341-2346.
[61] C.-F. Wang, X.-Y. Sun, M. Su, Y.-P. Wang, Y.-K. Lv, Electrochemical biosensors based on antibody, nucleic acid and enzyme functionalized graphene for the detection of disease-related biomolecules, Analyst. 145 (5) (2020) 1550-1562.
[62] J. G. S. Moo, A. Ambrosi, A. Bonanni, M. Pumera, Inherent Electrochemistry and Activation of Chemically Modified Graphenes for Electrochemical Applications, Chem. Asian J. 7 (4) (2012) 759-770.
[63] A. H. Loo, A. Bonanni, M. Pumera, Mycotoxin Aptasensing Amplification by using Inherently Electroactive Graphene-Oxide Nanoplatelet Labels, Chemelectrochem. 2 (5) (2015) 743-747.
[64] G. Qiu, Z. Gai, Y. Tao, J. Schmitt, G. A. Kullak-Ublick, J. Wang, Dual-Functional Plasmonic Photothermal Biosensors for Highly Accurate Severe Acute Respiratory Syndrome Coronavirus 2 Detection, ACS Nano. 14 (5) (2020) 5268-5277.
[65] A. H. Loo, A. Bonanni, M. Pumera, Thrombin aptasensing with inherently electroactive graphene oxide nanoplatelets as labels, Nanoscale. 5 (11) (2013) 4758-4762.
[66] A. Bonanni, A. Ambrosi, M. Pumera, On Oxygen-Containing Groups in Chemically Modified Graphenes, Chem. Eur. J. 18 (15) (2012) 4541-4548.
[67] S. Pei, H.-M. Cheng, The reduction of graphene oxide, Carbon. 50 (9) (2012) 3210-3228.
[68] Z. Xu, X. Lei, Y. Tu, Z.-J. Tan, B. Song, H. Fang, Dynamic Cooperation of Hydrogen Binding and π Stacking in ssDNA Adsorption on Graphene Oxide, Chem. Eur. J. 23 (53) (2017) 13100-13104.
[69] B. Liu, S. Salgado, V. Maheshwari, J. Liu, DNA adsorbed on graphene and graphene oxide: Fundamental interactions, desorption and applications, Curr. Opin. Colloid Interface Sci. 26 (2016) 41-49.
[70] H. Lei, L. Mi, X. Zhou, J. Chen, J. Hu, S. Guo, Y. Zhang, Adsorption of double-stranded DNA to graphene oxide preventing enzymatic digestion, Nanoscale. 3 (9) (2011) 3888-3892.
[71] E. Desimoni, B. Brunetti, Presenting Analytical Performances of Electrochemical Sensors. Some Suggestions, Electroanalysis. 25 (7) (2013) 1645-1651.